




Threshold versus intensity functions in two-colour automated perimetry

Matthew P. Simunovic^{1,2} , Kristina Hess^{1,3} , Neil Avery² and Zaid Mammo² 

¹Save Sight Institute, Discipline of Ophthalmology, University of Sydney, Sydney, Australia, ²Retinal Unit, Sydney Eye Hospital, Sydney, Australia, and

³Department of Ophthalmology, University of Bonn, Bonn, Germany

Citation information: Simunovic MP, Hess K, Avery N, & Mammo Z. Threshold versus intensity functions in two-colour automated perimetry. *Ophthalmic Physiol Opt* 2021; 41: 157–164. <https://doi.org/10.1111/opo.12743>

Keywords: light adaptation, perimetry, retina, selective perimetry, threshold versus intensity functions

Correspondence: Matthew P. Simunovic
E-mail address:
matthew.simunovic@sydney.edu.au

Received: 4 June 2020; Accepted: 31 August 2020; Published online: 16 October 2020

Abstract

Purpose: Two-colour computerised perimetry is a technique developed for assessing cone- and rod-function at fixed background luminances in retinal disease. However, the state of adaptation during testing is unknown but crucial in the interpretation of results. We therefore aimed to determine the adaptational state of rod- and cone-mechanisms in two-colour perimetry.

Methods: Sensitivity to 480 nm (blue) and 640 nm (red) Goldmann size V targets was determined for 10 normal subjects aged 16 to 46 years at 17 locations in the central 60 degrees of the visual field under scotopic conditions and then from $-1.5 \log \text{cd m}^{-2}$ to $2 \log \text{cd m}^{-2}$ (white background) in 0.5 log unit steps. Data were fitted with threshold versus intensity (tvi) functions of the form $\log T = \log T_0 + \log ((A + A_0)/A_0)^n$.

Results: No clear rod-cone break was observed for 640 nm stimuli. For 480 nm stimuli, transition from rod-detection to cone-detection occurred at mesopic illumination levels, where rod adaptation approached Weber behaviour. Cone detection mechanisms did not display Weber-like adaptation until the background luminance approached $1 \log \text{cd.m}^{-2}$. Diseases resulting in a “filter effect” - including disorders of the photoreceptors - are therefore predicted to affect sensitivity when rod function is probed with short-wavelength targets under scotopic conditions, but less so under mesopic conditions. Filter effects are similarly anticipated to affect cone function measured using long-wavelength targets under mesopic conditions (e.g., during microperimetry), but less so under photopic conditions.

Conclusions: Asymmetries in adaptation in automated two-colour perimetry are predicted to artefactually favour the detection of losses in rod sensitivity under scotopic conditions and cones under mesopic conditions.

Introduction

Two-colour automated perimetry is a tool initially developed in the 1980s for separating rod- and cone-mediated responses in patients with inherited retinal degenerations.^{1,2} It typically involves testing of the visual field with large short-wavelength (e.g., Goldmann size V, blue) \pm long-wavelength (e.g., Goldmann size V, red) targets under scotopic conditions to isolate the rods.^{1,2} Long-wavelength (e.g., Goldmann size V or III, red) targets presented on a white background under photopic conditions (typically 10 cd m^{-2}) are subsequently used to suppress the rods and

isolate the cones.^{1,2} Analysis of spectral sensitivities suggests that each of these paradigms isolates the mechanism of interest by at least 2 log units (20 dB) in normal observers (assuming scotopic perimetry is conducted with only short-wavelength targets; under scotopic conditions, long-wavelength targets at $>640 \text{ nm}$ isolate the cones poorly).³ However, testing at more than two wavelengths may be required to definitively determine the mechanism being probed in patients with retinal disease.³ Similarly, this technique may be cautiously extended to study cone- and rod-function under the mesopic conditions employed in microperimetry.³

It had previously been assumed that the visual system would demonstrate similar spectral sensitivity to the Commission Internationale de l'Éclairage (CIE) $V'\lambda$ (scotopic spectral sensitivity) function under scotopic perimetric conditions.^{1,2} Correspondingly, it has been implicitly assumed that the visual system would display similar sensitivity to the CIE $V\lambda$ (photopic spectral sensitivity) function under photopic perimetric conditions.^{1,2} However, spectral sensitivity for centrally presented targets on neutral adapting fields departs from the CIE $V\lambda$ function, reflecting detection by colour-opponent mechanisms.⁴ Simian perimetric data initially suggested that intrusion by colour-opponent mechanisms occurs in clinical perimetry.⁵ More recently, it has been demonstrated in humans that at extrafoveal locations, a luminance (M + L-cone) mechanism largely dictates behaviour under photopic conditions; however, at the very centre of the visual field, opponent processes contribute substantially to target detection.³ Similarly, the state of retinal adaptation in two-colour perimetry has been implicitly assumed to reflect data obtained at the fovea using different psychophysical techniques to those employed in modern computerised perimetry. With the notable exception of short-wavelength automated perimetry (SWAP),⁶ adaptation has been largely overlooked in the context of automated perimetric techniques to isolate rods from cones (and vice versa), such as two-colour perimetry. Whilst largely ignored, this remains an important issue because inequalities in adaptation may result in spurious conclusions regarding the selectivity of pathology when testing at fixed background luminances, as is the case in clinical testing.⁷ Because two-colour perimetry has been used to infer the selective effects (if any) of retinal pathology on the rod- and cone-mediated pathways, it is crucial to understand not only the mechanisms contributing to target detection, but also their state of adaptation.

In conventional white-on-white photopic perimetry, background luminances are deliberately chosen to be close to where Weber's law holds ("Weber adaptation"),^{8,9} as this helps to negate the effects of certain extraneous variables, such as pupil size (as outlined below). It will be noted, however, that some conjecture exists as to whether the commonly employed background luminance of 10 cd m^{-2} is sufficient to provide such adaptation.^{10,11} Leaving this latter issue aside, Weber's law states:

$$K = \Delta I / I$$

where K is a constant and ΔI is the change in luminance required for the subject to see the target against a background of luminance I . Weber's law predicts that phenomena which exert a so-called "filter effect" (i.e., which simultaneously and equally attenuate the target and background luminance), such as pupil size and media

absorption, will not affect the recorded threshold unless they bring the background luminance to levels where Weber's law breaks down.⁸ In conventional white-on-white perimetry, where we want to avoid variations in sensitivity through these so-called "filter effects", using background luminances that place the visual system in a state where Weber's law holds is advantageous. However, tests that employ lower luminance levels (i.e., below those where Weber's law holds) will be vulnerable to such perturbations, and sensitivity estimates will decrease as a consequence of processes that lead to an increased "filter effect".⁷ Models of sensitivity loss from receptor and post-receptor pathology developed by Hood and colleagues anticipate that receptor defects (so-called "d₁ loss" and "d₂ loss") will result in a "filter effect".¹² This is reflected by an upwards and rightwards shift of the threshold versus intensity (tvi) curve. Post-receptor pathology ("d₃ loss"), by contrast, is predicted to result in an upwards translation of the curve. We reasoned that adaptational state has particular relevance to two-colour perimetry, where rod sensitivity is probed at absolute threshold (i.e., where threshold is independent of background luminance), whilst cone sensitivity is determined at higher light levels, where some degree of adaptation is anticipated.

With renewed interest in functional biomarkers for inherited retinal disease as the result of emerging treatments, it is crucial to explore precisely how the results of two-colour perimetry should be interpreted.³ Although the mechanisms governing stimulus detection under the conditions used in two-colour perimetry have been established in simians⁵ and humans,³ their adaptational state under such conditions remains unknown. We therefore aimed to generate threshold versus intensity (tvi) functions for short- and long-wavelength targets at luminance levels spanning those employed for clinical two-colour perimetry to address this question. We hypothesised that Weber's law would break down for cones under the mesopic illumination conditions typically employed with clinical microperimetry (and therefore at lower, scotopic light levels). Furthermore, we predicted that Weber's law would hold for rods and cones under the photopic conditions used in conventional white-on-white/red-on-white perimetry. In turn, we reasoned that adaptational asymmetries introduced through clinical testing at a fixed background luminance would be predicted to lead to biases in the detection of functional defects by two-colour perimetry in disease processes which lead to a "filter effect".

Methods

A total of 10 subjects aged 16 to 45 years undertook this study, which was approved by the Institutional Review Board and adhered to the tenets of the Declaration of

Helsinki. All subjects had a corrected visual acuity of 6/6 (logMAR 0.0) or better, normal ophthalmic examinations and had normal red-green colour vision as screened by the Ishihara Test for Colour Blindness. All subjects were in good systemic health and were not taking any medications with known ocular or neurological side-effects. Before testing, the subject's pupils were dilated with 1% tropicamide and 2.5% phenylephrine. Testing was conducted monocularly in the right eye with the MonCVOne Perimeter (MetroVision, www.metrovision.fr) in a specially designed dark-room with calibration checks performed with an Ocean Insight USB4000 spectroradiometer (www.oceaninsight.com). The MonCVOne perimeter consists of a white Ganzfeld bowl of 30 cm radius; LEDs provide the background illuminant of the instrument, and an optical system is used to project LED stimuli onto the bowl. Testing commenced under scotopic conditions after 20 min of dark adaptation, and a total of 17 points in the central 60° of the visual field were tested. These included the point of fixation (Cartesian coordinates 0°, 0°) as well as stimuli along the diagonal points included in the 30-2 Humphrey Visual Field Test ($\pm 3^\circ$, $\pm 3^\circ$; $\pm 9^\circ$, $\pm 9^\circ$; $\pm 15^\circ$, $\pm 15^\circ$; $\pm 21^\circ$, $\pm 21^\circ$; see Figure 1).³ Threshold was determined for blue (480 nm) and red (640 nm) Goldmann size V (1.7° diameter circular) targets, which are produced by placing narrow-band interference filters in the optical pathway of the projected stimuli (10 nm full-width at half-maximum). Threshold was determined using a 4-2-2 dB interleaved staircase algorithm similar to that described previously.^{3,13} Two test runs were performed prior to commencement of

the experiment and breaks were permitted between tests, according to the subject's preference. Once measurements were completed under scotopic conditions, a neutral (white) background was added at $-1.5 \log$ (photopic) cd m^{-2} and testing repeated for both stimulus wavelengths (CIE 1931 chromaticity diagram co-ordinates of the background $x = 0.329$, $y = 0.338$; constant down to $-2.9 \log \text{cd m}^{-2}$). Background intensity was subsequently increased in 0.5 log unit increments up to $2 \log \text{cd m}^{-2}$, and testing was repeated at each intensity for each stimulus wavelength. After the completion of testing, background and threshold values were converted into trolands, based upon averaged automated pupil size measurements using the MonCVOne perimeter and known luminance values. Data were then fitted using a least-squares method in GraphPad Prism (www.graphpad.com) with tvI curves of the form:

$$\log T = \log T_0 + \log((A + A_0)/A_0)^n$$

where T is threshold, T_0 is absolute threshold, A is background intensity, A_0 is the "dark-light" constant and n is a gain constant ($n = 0.5$ reflects DeVries-Rose adaptation, $n = 1$ reflects Weber adaptation and $n > 1$ reflects saturation).¹⁴ The best fitting model, in terms of T_0 , A_0 , and n , was based upon the adjusted R^2 at each fitted test eccentricity. Although subjective appearance of stimuli has been used to identify detecting mechanisms,¹⁵ we assumed their identity based upon previous experiments of spectral sensitivity at fixed background intensities under scotopic, mesopic and photopic conditions.³ Where our previous experiments suggest transition from rod- to M + L detection (and from M + L detection to M vs L detection at the fovea) between these fixed background light levels, the model was constrained to assume that transition from one mechanism to another occurred at an intermediate light level. In the case of long-wavelength scotopic test data outside of fixation, we assumed equal sensitivity in rods and cones to the stimulus.³ For the purposes of analysis, we combined data from the same eccentricities within superonasal, supero-temporal, infero-nasal and infero-temporal fields, which thus implicitly assumes near-identical adaptation and transitions between mechanisms in these quadrants.

Results

The average total testing time was 90 min. The average values for T_0 , A_0 and n at each stimulus location for each target wavelength are summarised in Table 1. As anticipated, cone-mediated values for T_0 were lowest for foveally-presented targets, as was A_0 , the value for n at the point of fixation for the M + L mechanism approached 1. However, it was on average slightly lower at the more peripheral

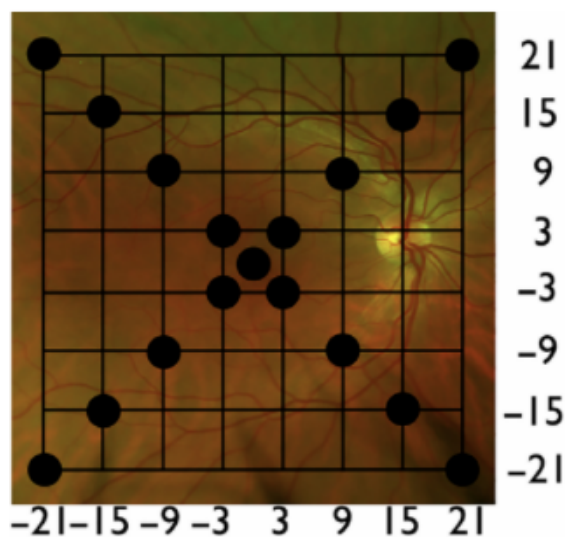


Figure 1. Perimetric test locations (black circles) projected onto a fundus image of a normal patient (target size not to scale). Axes represent eccentricity in degrees.

Table 1. Summary of values for T_0 and A_0 at fixation and averaged at $\pm 3^\circ$, $\pm 3^\circ$, $\pm 9^\circ$, $\pm 9^\circ$, $\pm 15^\circ$, $\pm 15^\circ$, $\pm 21^\circ$, $\pm 21^\circ$. Values are in log triand.* Constrained to be equal to the value for the red stimulus

Location	Mechanism	Red	Blue
Fixation	Rods	NA	$T_0 = -3.3$
	Cones	$T_0 = -2.2$, $A_0 = 1.0$ $n = 0.94$	$T_0 = -2.5$, $A_0 = 1.0$ $n = 0.94$
$\pm 3^\circ, \pm 3^\circ$	Rods	$T_0 = -1.9$, $A_0 = 1.6$ $n = 0.74$	$T_0 = -2.3$, $A_0 = 1.2$ $n = 0.73$
	Cones	*	$T_0 = -4.2$, $A_0 = -1.5$ $n = 0.70$
$\pm 9^\circ, \pm 9^\circ$	Rods	$T_0 = -2.1$, $A_0 = 1.3$ $n = 0.79$	$T_0 = -2.4$, $A_0 = 1.3$ $n = 0.83$
	Cones	*	$T_0 = -4.2$, $A_0 = -0.94$ $n = 0.89$
$\pm 15^\circ, \pm 15^\circ$	Rods	$T_0 = -1.8$, $A_0 = 1.3$ $n = 0.82$	$T_0 = -2.4$, $A_0 = 1.3$ $n = 0.95$
	Cones	*	$T_0 = -4.2$, $A_0 = -1.1$ $n = 0.83$
$\pm 21^\circ, \pm 21^\circ$	Rods	$T_0 = -1.6$, $A_0 = 1.3$ $n = 0.85$	$T_0 = -2.3$, $A_0 = 1.3^*$ $n = 0.94$
	Cones	*	$T_0 = -4.1$, $A_0 = -1.2$ $n = 0.82$
		$T_0 = -1.4$, $A_0 = 1.5$ $n = 0.92$	$T_0 = -1.9$, $A_0 = 1.5^*$ $n = 0.94$

*Rod and cone thresholds for 640 nm targets co-incident under scotopic conditions.³

stimulus locations, in keeping with observations in simians.⁵ Similarly – and consistent with previous observations – the value for n was less than 1 for the rod system¹⁶ and the M vs L-opponent mechanism.^{14,17} For 640 nm Goldmann size V targets presented under scotopic conditions, rods and cones were assumed to be equally sensitive, except at the point of fixation³ (though it will be noted that preceding bleaching protocols can be used to suppress rod responses and explore absolute cone threshold).¹⁸ Threshold versus intensity functions for background luminances between $-1.5 \log \text{cd m}^{-2}$ and $2 \log \text{cd m}^{-2}$ measured at the point of fixation were biphasic (Figure 2). Based upon previous experiments to determine spectral sensitivities at fixed intensities under scotopic, mesopic and photopic conditions, we conclude that this results from a transition between detection by an additive M- + L-cone mechanism at lower luminances to an opponent M- vs L-cone mechanism at higher luminances.³ At more peripheral locations (Figure 3a-d) for backgrounds between $-1.5 \log \text{cd m}^{-2}$ and $2 \log \text{cd m}^{-2}$, increment threshold curves for 640 nm targets were monophasic, and reflect detection by an additive M + L-cone mechanism.³ Increment threshold functions for 480 nm Goldmann size V targets, by contrast, were best described by biphasic fits at all stimulus locations

(Figure 3a-d) with a break occurring at mesopic illuminations levels, except for the point of fixation where they were triphasic (Figure 1). Based again on our previous observations of spectral sensitivity at fixed background intensities, we conclude that the initial portion of the peripheral biphasic curves reflects detection by the rods and that the first break indicates transition to detection by the M + L-cone mechanism.³ This break was poorly defined at ($\pm 15^\circ$, $\pm 15^\circ$) and ($\pm 21^\circ$, $\pm 21^\circ$), where the model was constrained to fit two curves (the second having the same A_0 value as the parallel curve for the 640 nm target, as the same mechanism is assumed to govern detection).³ At the point of fixation, the rod-M + L-cone break was observed at lower mesopic background levels. Furthermore, a second break was found at the point of fixation at low photopic levels. This is consistent with transition from detection by the M + L-cone mechanism to the M vs L-opponent mechanism (Figure 2).³ The cone adaptation functions did not display Weber behaviour until the background luminance approached $1 \log \text{cd m}^{-2}$.

Discussion

Previous experiments using fixed background intensities have demonstrated that scotopic perimetry with blue Goldmann size V stimuli isolates the rods^{1,2} and red Goldmann size V stimuli presented on a white $1 \log \text{cd m}^{-2}$ background isolates cone-mediated mechanisms.³ The current experiments establish the state of retinal adaptation under these and intermediate conditions. Our adaptation data have important – although easily overlooked – implications for the interpretation of results of tests performed under clinical conditions using fixed background intensities.

As stated earlier, so-called filter effects may alter thresholds when testing under conditions where Weber's law does not hold.^{10,11} The most obvious "filter effects" are pre-receptoral in nature and include variations in pupil size and ocular media transmission. It has been proposed that receptor disease will result in a filter effect (d1 or d2 loss) and optic nerve disease will result in so-called d3 loss.¹² However, the empirical evidence to date from a variety of psychophysical approaches suggests that "retinal" and "optic nerve" disease can produce isolated d1/d2 or d3 loss in some patients, whilst in others, mixed loss occurs (although d1/d2 or d3 mechanism loss respectively may predominate).^{7,12,19,20} This may reflect the fact that diseases of the outer retina also result in inner retinal remodeling²¹ and that optic neuropathies (such as glaucoma) may also involve the outer retina/photoreceptors.²² For example, previous studies of absolute threshold and low photopic threshold testing at limited fixed locations, or for large fields, in glaucoma have illustrated that a filter effect may

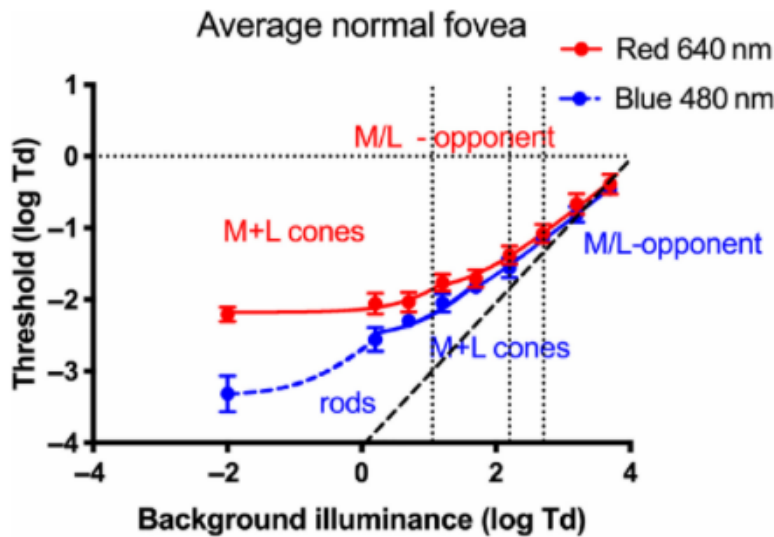


Figure 2. Threshold versus background retinal illuminance at the point of fixation for Goldmann Size V targets (480 nm - blue dots; 640 nm - red dots) presented on a white background. Data are fitted with tvI curves (see text). Vertical dashed lines from left to right indicate retinal illuminances for standard mesopic perimetry (3.2 cd m^{-2} background) and standard photopic perimetry (10 cd m^{-2} background) through a natural and a dilated pupil, respectively. The diagonal dashed line indicates Weber adaptation.

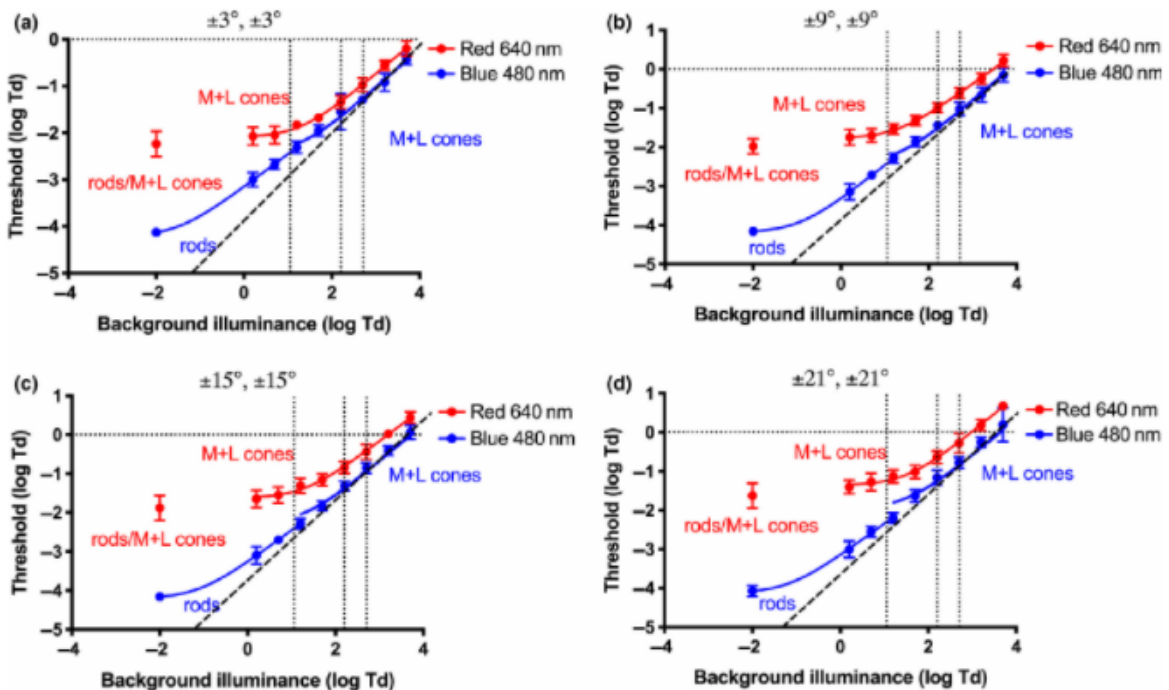


Figure 3. Threshold versus background retinal illuminance averaged at ($\pm 3^\circ, \pm 3^\circ$; a), ($\pm 9^\circ, \pm 9^\circ$; b), ($\pm 15^\circ, \pm 15^\circ$; c), ($\pm 21^\circ, \pm 21^\circ$; d) for Goldmann Size V targets presented on a white background (480 nm - blue dots; 640 nm - red dots). Data are fitted with tvI curves (see text). Vertical dashed lines from left to right indicate retinal illuminances for standard mesopic perimetry (3.2 cd m^{-2} background) and standard photopic perimetry (10 cd m^{-2} background) through a natural and a dilated pupil, respectively. The diagonal dashed line indicates Weber adaptation.

be at play in glaucomatous optic neuropathy.^{23,24} This is despite the fact that optic nerve disease has been hypothesised to result in so-called d3 loss, which is proposed to result in an upwards translation of the tvi curve. The filter effect has also previously been invoked to account for the apparent vulnerability of the S-cone system to pathology.^{7,25} The hypothesis has been directly tested by Kalloniatis and Harwerth with respect to S-cone mediated sensitivity loss in primates, where increment threshold testing was performed both before, and after, photic insult.⁷ Their study concluded that the filter-effect could account for a significant proportion (but not all) of S-cone deficits measured psychophysically under conditions where background luminance is fixed.⁷ In contrast, Greenstein and colleagues²⁶ increment threshold data in patients with retinitis pigmentosa (genotype unknown) and diabetic retinopathy do not directly support a filter-like effect in the S-cone system, although their clinical approach could not cover the same extensive range of background conditions employed by Kalloniatis and Harwerth.⁷ In clinical perimetry, there are limited data on the applicability of the d1/d2 and d3 models of sensitivity loss. Seiple and colleagues²⁷ found that 8 of 15 retinitis pigmentosa patients (genotype unknown) demonstrated losses in photopic perimetric sensitivity consistent with d1 loss; those with diabetic macular oedema demonstrated d3 loss. Herse¹⁹ employed Medmont perimetry to study non-exudative age-related macular degeneration (ARMD) and glaucoma using the tvi technique: the results supported a d1 mechanism loss in non-exudative ARMD and a d3 mechanism loss in glaucoma.

For the case of two-colour perimetry with Goldman size V stimuli, the scotopic portion of testing with a short wavelength target will be vulnerable to variations introduced via filter effects. Under mesopic conditions where the rods display Weber-like adaptation, their sensitivity is predicted to be largely independent of such filter effects.³ For long wavelength targets presented under mesopic conditions, cone-mediated sensitivity will be vulnerable to so-called filter effects. However, for photopic perimetric conditions, such as the commonly employed $1 \log \text{cd.m}^{-2}$ white background, our results suggest that cone sensitivity will be largely independent of filter effects as their adaptation approaches Weber behaviour at this luminance (unless of course the “filter” effectively reduces the background luminance to levels below that which Weber’s law holds). It will be noted that microperimetric approaches to two-colour perimetry may either employ mesopic or scotopic backgrounds.²⁸ In contrast to the approach generally employed with Ganzfeld-bowl based perimeters,^{1,2} microperimeters employ Goldman size III stimuli. Although our study is limited in not directly determining thresholds for Goldmann size III stimuli, reduction in stimulus size is predicted to result in a vertical translation of the tvi curve, i.e., T_0 will increase, but A_0 and n are anticipated to be unaltered. Therefore, identical caveats with respect to fixed luminances, as outlined above, are anticipated to apply to both Goldman size V and size III stimuli.

If not interpreted correctly, non-specific changes might be mistaken for selective impairment of one class of photoreceptor when fixed background intensities are used.

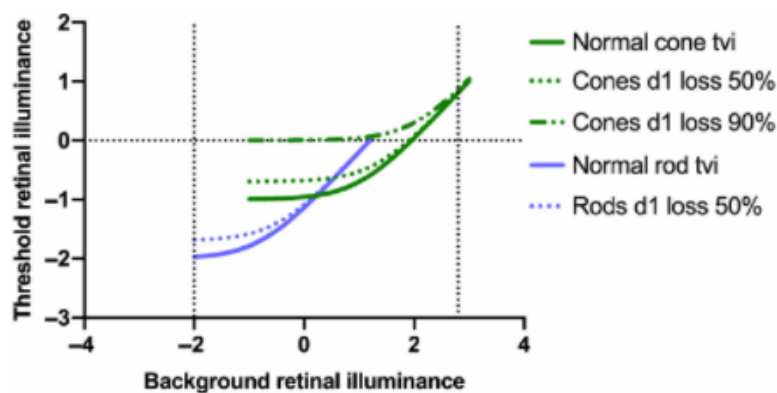


Figure 4. Predicted “d1” sensitivity loss (relative log luminance) versus background intensity (relative log luminance) depicted as a dotted line for rods (purple) and cones (green). Normal sensitivity is plotted as a solid line for rods (purple) and cones (green). d1 sensitivity loss results in equal upward and rightward translation of the tvi curve such that the Weber portions of the adaptation curves are co-incident (dotted and dot-dash lines). Consequently, tests performed under conditions where Weber’s law holds will not uncover this sensitivity loss (right vertical dotted line), whilst tests conducted at, and near, absolute threshold will detect such losses (left vertical dotted line). See text for details.

Furthermore, it may even lead to misidentification of the predominately affected mechanism. As noted above, depression in sensitivity from disease processes involving the photoreceptors, including their loss and dysfunction (regardless of mechanism; so-called “d₁ loss” or “d₂ loss”)¹² are predicted to have a “filter effect” on tvi functions. Such losses lead to identical geometric changes in T_0 and A_0 (i.e., arithmetic changes when converted to log₁₀ units). Therefore, a hypothetical non-selective generalised loss of 50% of the rod- and cone-function will be predicted to result in a 0.3 log unit upwards and rightward translation of the tvi function (see Figure 4). Thus, we would anticipate a decrease in sensitivity of 0.3 log units for 480 nm targets under scotopic conditions, but not for 640 nm targets presented against a white background at 1 log cd.m⁻². Furthermore, in instances of disease preferentially involving cones, there may still be apparent selective loss of rod function with two-colour perimetry. For example, if we have a 90% loss of cone function, but a 50% loss of rod function, then the same testing conditions would paradoxically demonstrate selective rod involvement (Figure 4). Although testing cone function at absolute threshold is superficially attractive, in this context it provides poor isolation except at the point of fixation.³ Consequently, care needs to be taken when attempting to determine the selectivity of disease processes using two-colour perimetry under fixed background luminances because of the observed inequalities in adaptation.

Our results therefore suggest that disease processes resulting in filter effect — either at a pre-receptor (e.g., ocular media, pupil size) or at the receptor level would result in preferential losses in sensitivity when assessed at absolute threshold. Because two-colour perimetric paradigms typically assess rod function at absolute threshold, and cone function where Weber’s law holds, this technique will artefactually favour the detection of rod abnormalities. The differential effects of adaptation might account for the observation that rod thresholds — as assessed by two-colour perimetry — are disproportionately affected by Stargardt’s disease.²⁹ This is despite evidence to suggest that mutations in the causative ABCA4 gene impair cones more than rods,³⁰ and that sensitivity loss for cones is greater than rods at absolute threshold.³¹

In summary, conventional two-colour perimetry — in which scotopic sensitivity is first determined with short- and long-wavelength stimuli, followed by photopic testing against a white 10cd.m⁻² background — places the rods at a selective disadvantage. Our results suggest that further exploration of d1/d2 and d3 mechanism loss is warranted in humans with retinal disease to better understand the mechanisms of topographical losses in cone- and rod-mediated function. This could be combined with modern imaging techniques, such as optical coherence tomography

and adaptive optics imaging³² and correlated with molecular genetics in the case of inherited retinal diseases.

Disclosures

Grant Support from a Foundation Fighting Blindness Career Development Award (MPS: CD-CL- 0816-0710-SYD).

Author contribution

Kristina Hess: Investigation (supporting). **Neil Avery:** Investigation (supporting). **Zaid Mammo:** Investigation (supporting).

References

- Jacobson SG, Apathy PP & Parel JM. Rod and cone perimetry: computerized testing and analysis. In: *Principles and practice of clinical electrophysiology of vision* (Marshall DK, ed). St. Louis: Mosby Year Book Inc, 1991.
- Jacobson SG, Voigt WJ, Parel JM et al. Automated light- and dark-adapted perimetry for evaluating retinitis pigmentosa. *Ophthalmology* 1986; 93: 1604–1611.
- Simunovic MP, Moore AT & MacLaren RE. Selective automated perimetry under photopic, mesopic, and scotopic conditions: detection mechanisms and testing strategies. *Transl Vis Sci Technol* 2016; 5: 10.
- Sloan LL. The effect of intensity of light, state of adaptation of the eye, and size of photometric field on the visibility curve. *Psychol Monogr* 1929; 38: 1–87.
- Harwerth RS, Smith EL 3rd & DeSantis L. Mechanisms mediating visual detection in static perimetry. *Invest Ophthalmol Vis Sci* 1993; 34: 3011–3023.
- Sample PA, Johnson CA, Haegerstrom-Portnoy G & Adams AJ. Optimum parameters for short-wavelength automated perimetry. *J Glaucoma* 1996; 5: 375–383.
- Kalloniatis M & Harwerth RS. Differential Adaptation of Cone Mechanisms Explains the Preferential Loss of Short-Wavelength Cone Sensitivity in Retinal Disease. In: *Colour Vision Deficiencies IX* (Drum B, Verriest G, editor), Springer: Netherlands, 1989; pp. 353–364.
- Bierings R, de Boer MH & Jansonius NM. Visual performance as a function of luminance in glaucoma: the De Vries-Rose, Weber’s, and Ferry-Porter’s Law. *Invest Ophthalmol Vis Sci* 2018; 59: 3416–3423.
- Heuer DK, Anderson DR, Feuer WJ & Gressel MG. The influence of decreased retinal illumination on automated perimetric threshold measurements. *Am J Ophthalmol* 1989; 108: 643–650.
- Fankhauser F. Problems related to the design of automatic perimeters. *Doc Ophthalmol* 1979; 47: 89–139.
- Fankhauser F. Background illumination and automated perimetry. *Arch Ophthalmol* 1986; 104: 1126.

12. Hood DC & Greenstein V. Models of the normal and abnormal rod system. *Vision Res* 1990; 30: 51–68.
13. Simunovic MP, Cullerne A, Colley A & Wilson TD. How well does color perimetry isolate responses from individual cone mechanisms? *J Glaucoma* 2004; 13: 22–27.
14. Kalloniatis M & Harwerth RS. Spectral sensitivity and adaptation characteristics of cone mechanisms under white-light adaptation. *J Opt Soc Am A* 1990; 7: 1912–1928.
15. King-Smith PE & Carden D. Luminance and opponent-color contributions to visual detection and adaptation and to temporal and spatial integration. *J Opt Soc Am* 1976; 66: 709–717.
16. Sharpe LT, Fach C, Nordby K & Stockman A. The incremental threshold of the rod visual system and Weber's law. *Science* 1989; 244: 354–356.
17. King-Smith PE & Kranda K. Photopic adaptation in the red-green spectral range. *Vision Res* 1981; 21: 565–572.
18. Stabell B & Stabell U. Absolute spectral sensitivity at different eccentricities. *J Opt Soc Am* 1981; 71: 836–840.
19. Herse P. An application of threshold-versus-intensity functions in automated static perimetry. *Vision Res* 2005; 45: 461–468.
20. Seiple WH, Holopigian K, Greenstein VC & Hood DC. Sites of cone system sensitivity loss in retinitis pigmentosa. *Invest Ophthalmol Vis Sci* 1993; 34: 2638–2645.
21. Jones BW, Pfeiffer RL, Ferrell WD, Watt CB, Marmor M & Marc RE. Retinal remodeling in human retinitis pigmentosa. *Exp Eye Res* 2016; 150: 149–165.
22. Nork TM. Acquired color vision loss and a possible mechanism of ganglion cell death in glaucoma. *Trans Am Ophthalmol Soc* 2000; 98: 331–363.
23. Glovinsky Y, Quigley HA, Drum B, Bissett RA & Jampel HD. A whole-field scotopic retinal sensitivity test for the detection of early glaucoma damage. *Arch Ophthalmol* 1992; 110: 486–490.
24. Drum B, Armaly MF & Huppert W. Scotopic sensitivity loss in glaucoma. *Arch Ophthalmol* 1986; 104: 712–717.
25. Simunovic MP. Acquired color vision deficiency. *Surv Ophthalmol* 2016; 61: 132–155.
26. Greenstein VC, Hood DC, Ritch R, Steinberger D & Carr RE. S (blue) cone pathway vulnerability in retinitis pigmentosa, diabetes and glaucoma. *Invest Ophthalmol Vis Sci* 1989; 30: 1732–1737.
27. Seiple W, Greenstein VC, Holopigian K, Carr RE & Hood DC. A method for comparing psychophysical and multifocal electroretinographic increment thresholds. *Vision Res* 2002; 42: 257–269.
28. Pfau M, Lindner M, Gliem M et al. Mesopic and dark-adapted two-color fundus-controlled perimetry in patients with cuticular, reticular, and soft drusen. *Eye* 2018; 32: 1819–1830.
29. Cideciyan AV, Swider M, Aleman TS et al. ABCA4 disease progression and a proposed strategy for gene therapy. *Hum Mol Genet* 2009; 18: 931–941.
30. Conley SM, Cai X, Makkia R, Wu Y, Sparrow JR & Naash MI. Increased cone sensitivity to ABCA4 deficiency provides insight into macular vision loss in Stargardt's dystrophy. *Biochim Biophys Acta* 2012; 1822: 1169–1179.
31. Collison FT, Fishman GA, McAnany JJ, Zernant J & Allikmets R. Psychophysical measurement of rod and cone thresholds in Stargardt disease with full-field stimuli. *Retina* 2014; 34: 1888–1895.
32. Phu J, Kalloniatis M, Wang H & Khuu SK. Optimising the structure-function relationship at the locus of deficit in retinal disease. *Front Neurosci* 2019; 13: 306.